Derivation of a continuum model and the energy law for moving contact lines with insoluble surfactants

Cite as: Phys. Fluids **26**, 062103 (2014); https://doi.org/10.1063/1.4881195
Submitted: 19 March 2014 . Accepted: 20 May 2014 . Published Online: 05 June 2014

Zhen Zhang, Shixin Xu, and Weiqing Ren

PHYSICS OF FLUIDS **26**, 062103 (2014)

Derivation of a continuum model and the energy law for moving contact lines with insoluble surfactants

Zhen Zhang,[1,a)] Shixin Xu,[1,b)] and Weiqing Ren[1,2,c)]
[1]*Department of Mathematics, National University of Singapore, Singapore 119076*
[2]*Institute of High Performance Computing, Agency for Science, Technology and Research, Singapore 138632*

(Received 19 March 2014; accepted 20 May 2014; published online 5 June 2014)

A continuous model is derived for the dynamics of two immiscible fluids with moving contact lines and insoluble surfactants based on thermodynamic principles. The continuum model consists of the Navier-Stokes equations for the dynamics of the two fluids and a convection-diffusion equation for the evolution of the surfactant on the fluid interface. The interface condition, the boundary condition for the slip velocity, and the condition for the dynamic contact angle are derived from the consideration of energy dissipations. Different types of energy dissipations, including the viscous dissipation, the dissipations on the solid wall and at the contact line, as well as the dissipation due to the diffusion of surfactant, are identified from the analysis. A finite element method is developed for the continuum model. Numerical experiments are performed to demonstrate the influence of surfactant on the contact line dynamics. The different types of energy dissipations are compared numerically. © *2014 AIP Publishing LLC*. [http://dx.doi.org/10.1063/1.4881195]

I. INTRODUCTION

Modeling and simulation of multi-phase flows with surfactants have attracted much attention from the scientific community in recent years.[1–8] This is mainly because of their many industrial applications, e.g., industrial emulsification, liquid/liquid extraction and hydrodesulfurization of crude oil, polymer blending and plastic production, cleaning using detergent, micro fluidics, etc.[9–16] In this work, we give a mathematical derivation of a continuum model for the dynamics of two immiscible fluids with moving contact lines and insoluble surfactants. We will focus on the conditions on the fluid interface, the boundary condition for the slip velocity on the solid wall, and the condition for the dynamic contact angle. The derivation is based on the consideration of thermodynamics and the energy law of the dynamical system.

When two immiscible fluids are placed in a container or on a substrate, the line where the interface of the two fluid phases intersects the solid container or the substrate is called the contact line. The equilibrium configuration of the static contact line was the topic of classical work of Young, Laplace, and Gauss,[17] and is described by Young's equation

$$\gamma \cos\theta_Y = \gamma_2 - \gamma_1, \tag{1}$$

which relates the three coefficients of interfacial tension to the contact angle formed by the fluid interface with the solid surface (see Fig. 1). The moving contact line problem, however, has for many years remained an issue of controversy and debate. The difficulty stems partly from the fact that classical hydrodynamic equations, the Navier-Stokes equations, coupled with the conventional no-slip boundary condition predict a singularity for the stress that results in a non-physical divergence

[a)]Electronic mail: matzz@nus.edu.sg
[b)]Electronic mail: matxs@nus.edu.sg
[c)]Author to whom correspondence should be sent. Electronic mail: matrw@nus.edu.sg

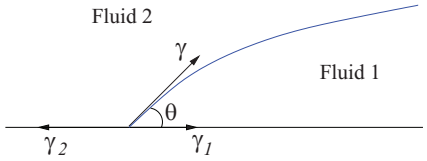

FIG. 1. Two immiscible fluids in contact with a solid substrate. γ, γ_1, and γ_2 are the surface tension coefficients of the three interfaces; θ is the contact angle of the fluid interface with the solid wall.

for the energy dissipation rate.[18,19] We refer to the review articles[20–23] and the monographs[24–26] for the discussions of the current status of the moving contact line problem.

In a recent work, Ren *et al.* derived boundary conditions for the moving contact line problem based on thermodynamics principles.[27,28] The macroscopic thermodynamics was used to limit the form of the boundary conditions, then the detailed constitutive relations in these boundary conditions were computed from molecular dynamics simulations. Two boundary conditions were derived, one for the slip velocity of the fluids on the solid wall, and the other for the dynamic contact angle θ_d. In two dimensions, these conditions are

$$\mathbf{t} \cdot \tau_d \cdot \mathbf{n} = f_i(u_s), \quad \text{on } \Gamma_i, \tag{2a}$$

$$\gamma\,(\cos\theta_d - \cos\theta_Y) = f_{CL}(u_l), \quad \text{on } \Lambda, \tag{2b}$$

where u_s and u_l are the slip velocity of the fluids and the normal velocity of the contact line, respectively; the left-hand side of (2a) is the shear stress of the fluids, Γ_i (i = 1,2) and Λ are the solid surface and the contact line, respectively. The functions $f_i(u)$ and $f_{CL}(u)$ satisfy the constraints

$$u \cdot f_i(u) \leqslant 0, \quad u f_{CL}(u) \leqslant 0, \tag{3}$$

for any velocity u. The explicit form of these two functions should be calibrated by experiments or microscopic measurements such as molecular dynamics. When the function $f_i(u)$ is linear, i.e., $f_i(u) = -\beta_i u$, the boundary condition (2a) reduces to the Navier boundary condition. Even though the idea used in these earlier work is quite simple, this is a rather powerful approach and it is useful for many other problems.

In this work, we extend these results to systems with insoluble surfactants. Insoluble surfactants concentrate on the fluid interface. The surface tension of the interface becomes a variable, and it depends on the local concentration of the surfactant. This in turn influences the contact line dynamics. A complete description of the system requires modeling the coupled dynamics of the surfactant and the fluids.

Some continuum models and numerical methods for multiphase flow with surfactants have been proposed in previous works.[2–5,7,8,29–31] The evolution equation of the surfactant along the fluid interface was derived by Stone[32] and Wong *et al.*[33] Various numerical methods, using the volume-of-fluid technique, the level set method, the immersed boundary method, the boundary integral method, etc., were also developed.[1–4,6–8,30,34–36] Most of these earlier works deal with closed interfaces without moving contact lines. An immersed boundary method was developed by Lai *et al.* for the study of the contact line dynamics with surfactant.[31] There, the unbalanced Young stress, which is due to the deviation of the dynamic contact angle from the static contact angle, was included in the momentum equation as a driving force. Recently, Xu and Ren developed a level-set method for the simulation of two-phase flows with moving contact lines and insoluble surfactants.[37]

In the current work, we give a mathematical derivation of a continuum model from the consideration of energy dissipations. Starting with the total free energy of the system, we use the approach proposed in Refs. 27 and 28 to derive both the static and the dynamic models in a variational framework. When the constitutive relations are linear, the continuum model derived here leads to the one used in previous work.[37]

Another objective of this work is to understand the mechanism of the energy dissipation of the dynamical system. From the analysis, we obtain the energy law for the continuum model and identify the different types of energy dissipations. These include the energy dissipation in the bulk

due to the viscous force, the energy dissipations along the solid surface and at the contact line due to the friction forces, and that on the fluid interface due to the diffusion of the surfactant.

This paper is organized as follows. We begin in Sec. II with the static problem. We derive the Young-Laplace equation for the fluid interface and the Young's relation for the contact angle in the presence of surfactant by minimizing the free energy. The analysis also gives the equilibrium condition for the surfactant concentration. In Sec. III, we discuss the dynamic problem from the viewpoint of thermodynamics. We obtain the interface condition, the slip condition along the solid wall, and the contact angle condition at the contact line. We also derive the energy law for the dynamics. A finite element method for the continuum model and numerical results are presented in Sec. IV. These results demonstrate the effect of surfactant on the contact line dynamics, and the different types of energy dissipations. Concluding remarks are made in Sec. V.

II. STATIC CONFIGURATION OF THE INTERFACE IN THE PRESENCE OF SURFACTANT

We begin with the situation of the static contact line. Consider a 3d droplet sitting on a 2d solid substrate. For simplicity, we consider the case in which the interface of the droplet can be parameterized by (x, y), the two coordinates on the solid wall, $z = z(x, y)$, where $(x, y) \in \Gamma_1$ and Γ_1 is the region occupied by the droplet on the solid wall.

We denote by $\mathbf{n}$ the unit vector normal to the interface pointing away from the droplet, $\mathbf{n}_b$ the unit vector normal to the solid wall in the outward direction. Along the contact line, which is denoted by Λ, we use $\mathbf{t}_l$ and $\mathbf{n}_l$ to denote the unit vectors on the solid surface that are tangent and normal to the contact line, respectively, and use $\mathbf{n}_s$ to denote the unit vector on the interface Γ that is normal to the contact line. These vectors are depicted in Fig. 2 and defined as follows:

$$\mathbf{t}_l = \frac{\mathbf{n} \times \mathbf{n}_b}{\|\mathbf{n} \times \mathbf{n}_b\|}, \quad \mathbf{n}_l = \frac{\mathbf{n}_b \times \mathbf{t}_l}{\|\mathbf{n}_b \times \mathbf{t}_l\|}, \quad \mathbf{n}_s = \frac{\mathbf{t}_l \times \mathbf{n}}{\|\mathbf{t}_l \times \mathbf{n}\|}. \tag{4}$$

Assume the fluid interface Γ is covered by insoluble surfactants, with concentration described by the function $c(x, y)$. Then the total free energy of the system is

$$E(z, c) = \int_{\Gamma_1} (\gamma_1 - \gamma_2)\, \mathrm{d}x\mathrm{d}y + \int_{\Gamma_1} e(c) J(z_x, z_y)\, \mathrm{d}x\mathrm{d}y, \tag{5}$$

where $e(c)$ is the energy density of the interface Γ, $J = \sqrt{1 + z_x^2 + z_y^2}$ is the Jacobian, and z_x and z_y are the partial derivatives of $z(x, y)$. The first term of (5) is the energy of the fluid-solid interface, and the second term is the energy of the fluid interface. The static configuration of the droplet and the concentration of the surfactant on the interface can be obtained by minimizing the above energy, under the constraints that the volume of the droplet is fixed and the total amount of surfactant is conserved,

$$\int_{\Gamma_1} z(x, y)\, \mathrm{d}x\mathrm{d}y = Q, \tag{6a}$$

$$\int_{\Gamma_1} c(x, y) J(z_x, z_y)\, \mathrm{d}x\mathrm{d}y = M. \tag{6b}$$

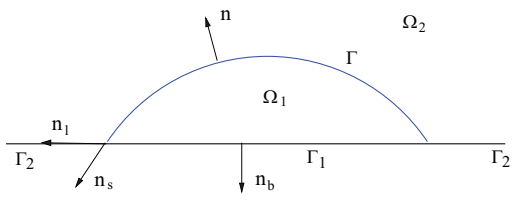

FIG. 2. Droplet on a solid substrate. Ω_1 and Ω_2 are the two fluid domains. Γ_1, Γ_2, and Γ are the three interfaces. $\mathbf{n}$ are $\mathbf{n}_b$ are the unit vectors normal to the fluid interface and the solid surface, respectively. $\mathbf{n}_l$ and $\mathbf{n}_s$ are the unit vectors normal to the contact line, and tangent to the solid surface and the fluid interface, respectively. $\mathbf{t}_l$ is the unit vector tangent to the contact line on the solid surface (not shown).

Moreover, $z(x, y) = 0$ holds at the contact line Λ.

The Euler-Lagrange equations lead to (see Appendix A)

$$(e(c) - e'(c)c)\kappa = \lambda, \tag{7a}$$

$$e'(c) = \mu, \tag{7b}$$

where the constants λ and μ are Lagrange multipliers associated with (6a) and (6b), respectively, and κ is the mean curvature of the interface: $\kappa = \nabla \cdot (J^{-1}z_x, J^{-1}z_y)$. The equilibrium contact angle of the interface, θ_Y, satisfies

$$\big(e(c) - e'(c)c\big)\cos\theta_Y = \gamma_2 - \gamma_1. \tag{8}$$

In (7a), the Lagrange multiplier λ serves as the pressure jump across the interface as will be seen in Sec. III. Equation (7b) simply states that the chemical potential must be constant when the system is at the equilibrium state. Obviously, when the function $e\prime(c)$ is strictly monotonic, this condition requires c to be constant which corresponds to a uniform distribution of the surfactant on the interface.

Using the definition of the surface tension,

$$\gamma(c) = e(c) - e'(c)c, \tag{9}$$

Eqs. (7a) and (7b) can be written as

$$\gamma(c)\kappa = \lambda, \tag{10a}$$

$$e'(c) = \mu, \tag{10b}$$

and the contact angle condition (8) has the usual form of the Young's relation:

$$\gamma(c)\cos\theta_Y = \gamma_2 - \gamma_1. \tag{11}$$

The Lagrange multipliers λ and μ are determined by the constraints in (6a) and (6b).

In the above derivation, we considered the situation when the interface can be parameterized using the two coordinates of the solid surface. We note that following the same procedure, the above equations can be derived for surfaces with general parameterizations.

III. DYNAMIC THEORY

Next we consider the dynamical problem. We derive mathematical models for the dynamics of the surfactant, the velocity of the fluids, and the evolution of the interface and the moving contact line. The derivation is based on the consideration of the second law of thermodynamics, in particular, the requirement that the rate of energy dissipation needs to be non-positive.

A. Dynamics of the surfactant on the fluid interface

The dynamical equation for the surfactant can be derived from the conservation law for the mass of the surfactant. This has been done in previous works.[32,33,38] For the sake of completeness, we give a brief derivation of this equation in the following. The background material on surface calculus can be found in Appendix B.

We consider insoluble surfactants which concentrate on the fluid interface. The conservation law for the mass of the surfactant states that the amount of surfactant is conserved on any element of the fluid interface:

$$\frac{\mathrm{d}}{\mathrm{d}t}\int_S c\,\mathrm{d}A + \int_{\partial S}\mathbf{J}_c\cdot\mathbf{n}_s\mathrm{d}l = 0, \tag{12}$$

where $S \subset \Gamma$ is the surface element, $c(\mathbf{x}, t)$ is the surfactant concentration, $\mathbf{J}_c$ is the mass flux, and $\mathbf{n}_s$ is the outward normal to ∂S in the tangent plane to the interface.

To derive the dynamical equation, it is more convenient to use the Lagrangian coordinate $\mathbf{X}$ to describe the interface. Let (s^1, s^2) be a parametrization of the interface at the initial time, then the interface at time t can be described as

$$\mathbf{x} = \mathbf{x}\left(\mathbf{X}(s^1, s^2), t\right), \quad (s^1, s^2) \in D. \tag{13}$$

Under this parametrization, the surface integral in (12) can be written as

$$\int_S c \, \mathrm{d}A = \int_{\delta D} c \, \|\mathbf{t}_1 \times \mathbf{t}_2\| \, \mathrm{d}s^1 \mathrm{d}s^2, \tag{14}$$

where δD is the subset of D corresponding to the surface element S, $\mathbf{t}_1$ and $\mathbf{t}_2$ are contravariant tangent vectors to the interface defined in (B1). Then using the identity (B8), the time derivative of the above integral can be written as

$$\frac{\mathrm{d}}{\mathrm{d}t} \int_S c \, \mathrm{d}A = \int_S \left(\frac{\mathrm{D}c}{\mathrm{D}t} + (\nabla_s \cdot \mathbf{u}) c \right) \mathrm{d}A, \tag{15}$$

where $\frac{\mathrm{D}c}{\mathrm{D}t}$ is the material derivative of c, and $\nabla_s \cdot \mathbf{u}$ is the surface divergence of the velocity field $\mathbf{u}$. The surface divergence is defined in (B6).

By using the surface divergence theorem (B7), the second term of (12) can be written as

$$\int_{\partial S} \mathbf{J}_c \cdot \mathbf{n}_s \, \mathrm{d}l = \int_S \nabla_s \cdot \mathbf{J}_c \, \mathrm{d}A, \tag{16}$$

where we have used the fact that $\mathbf{J}_c \cdot \mathbf{n} = 0$, since the flux of c is along the interface.

Combining (12), (15), and (16), we obtain

$$\int_S \left(\frac{\mathrm{D}c}{\mathrm{D}t} + (\nabla_s \cdot \mathbf{u}) c + \nabla_s \cdot \mathbf{J}_c \right) \mathrm{d}A = 0. \tag{17}$$

Since the surface segment S is arbitrary, we arrive at the differential form of the conservation law for the surfactant:

$$\frac{\mathrm{D}c}{\mathrm{D}t} + (\nabla_s \cdot \mathbf{u}) c = -\nabla_s \cdot \mathbf{J}_c, \qquad \text{on } \Gamma \tag{18}$$

with the boundary condition

$$\mathbf{J}_c \cdot \mathbf{n}_s = 0, \qquad \text{on } \Lambda. \tag{19}$$

Equation (18) has been derived by Stone,[32] and later was recast by Wong *et al.*[33] It is an instance of the generalized Reynolds transport equation on surfaces.[38]

B. Continuum model for the moving contact line with surfactant

Next we derive the continuum model for the moving contact line in the presence of surfactant on the interface. The main results of this analysis are: (1) The form of the boundary conditions and the constraints on the constitutive relations in the continuum model, and (2) the energy law for the dynamics. We derive these results from the consideration of thermodynamics, in particular, the energy dissipations in the dynamical process. This approach was used by Ren *et al.*[27] to derive the boundary conditions for the moving contact line problems without surfactants.

We consider the relaxation dynamics of a 3d droplet on a 2d solid surface. We assume the solid substrate is at rest. The total free energy of the system is

$$F = \sum_{i=1,2} \int_{\Omega_i} \frac{1}{2} \rho_i |\mathbf{u}|^2 \, \mathrm{d}\mathbf{x} + (\gamma_1 - \gamma_2)|\Gamma_1| + \int_{\Gamma(t)} e(c) \, \mathrm{d}A, \tag{20}$$

where the first term is the kinetic energy of the fluids, with ρ_i and $\mathbf{u}$ being the density and velocity of the fluids, respectively; the last two terms are the surface energy of the fluid-solid and the fluid-fluid interfaces, respectively.

We assume the fluids are iso-thermal and incompressible, so the dynamical equations in the bulk Ω_i $(i = 1, 2)$ have the usual form:

$$\rho_i(\partial_t \mathbf{u} + \mathbf{u} \cdot \nabla \mathbf{u}) = -\nabla p + \nabla \cdot \tau_d, \tag{21a}$$

$$\nabla \cdot \mathbf{u} = 0, \tag{21b}$$

where p is the pressure, and τ_d is the viscous stress. We assume the fluids are Newtonian, so τ_d is given by

$$\tau_d = \eta_i \left(\nabla \mathbf{u} + (\nabla \mathbf{u})^\top\right), \tag{22}$$

where η_i $(i = 1, 2)$ are the viscosity of the fluids.

Next we consider the dissipation rate for the energy (20). A straightforward calculation using the dynamical equations (18) and [(21a) and (21b)] gives

$$\begin{aligned}\frac{\mathrm{d}}{\mathrm{d}t}\sum_{i=1,2}\int_{\Omega_i}\frac{1}{2}\rho_i|\mathbf{u}|^2\,\mathrm{d}\mathbf{x} = &-\sum_{i=1,2}\int_{\Omega_i}\eta_i|\nabla\mathbf{u}|^2\,d\mathbf{x} + \sum_{i=1,2}\int_{\Gamma_i}\mathcal{P}\left(\tau_d\cdot\mathbf{n}_b\right)\cdot\mathbf{u}_s\,\mathrm{d}A\\ &+\int_{\Gamma}\mathbf{u}\cdot[\tau_d - p\mathbf{I}]\cdot\mathbf{n}\,\mathrm{d}A,\end{aligned} \tag{23}$$

$$\frac{\mathrm{d}}{\mathrm{d}t}\Big((\gamma_1-\gamma_2)\,|\Gamma_1|\Big) = \int_{\Lambda}(\gamma_1-\gamma_2)(\mathbf{u}\cdot\mathbf{n}_l)\,\mathrm{d}l, \tag{24}$$

and

$$\begin{aligned}\frac{\mathrm{d}}{\mathrm{d}t}\int_{\Gamma(t)}e(c)\,\mathrm{d}A &= \int_{\Gamma(t)}e(c)\nabla_s\cdot\mathbf{u}\,dA - \int_{\Gamma(t)}e'(c)\left(c\nabla_s\cdot\mathbf{u} + \nabla_s\cdot\mathbf{J}_c\right)\,\mathrm{d}A\\ &= \int_{\Gamma(t)}\left(\gamma(c)\kappa\mathbf{u}\cdot\mathbf{n} - \mathbf{u}\cdot\nabla_s\gamma(c) + e''(c)\nabla_s c\cdot\mathbf{J}_c\right)\,\mathrm{d}A\\ &\quad+\int_{\Lambda}\gamma(c)\mathbf{u}\cdot\mathbf{n}_s\,\mathrm{d}l,\end{aligned} \tag{25}$$

where $[\,\cdot\,]$ denotes the jump across the fluid interface, $\mathcal{P}$ is the projection operator on the solid surface: $\mathcal{P} = \mathbf{I} - \mathbf{n}_b \otimes \mathbf{n}_b$, $\mathbf{u}_s$ is the slip velocity of the fluids on the solid surface, and γ is the surface tension of the fluid interface as defined in (9). In deriving (25), we used the divergence theorem (B7), the orthogonality condition $\mathbf{J}_c \cdot \mathbf{n} = 0$ on the interface, the no-flux condition (19) at the contact line, and the no-penetration condition

$$\mathbf{u}\cdot\mathbf{n}_b = 0, \qquad \text{on } \Gamma_i. \tag{26}$$

Collecting the results in (23)–(25), we arrive at the following energy law:

$$\begin{aligned}\frac{\mathrm{d}F}{\mathrm{d}t} = &-\sum_{i=1,2}\int_{\Omega_i}\eta_i|\nabla\mathbf{u}|^2\,\mathrm{d}\mathbf{x} + \sum_{i=1,2}\int_{\Gamma_i}\mathcal{P}\left(\tau_d\cdot\mathbf{n}_b\right)\cdot\mathbf{u}_s\,\mathrm{d}A\\ &+\int_{\Gamma(t)}\mathbf{u}\cdot\Big\{[\tau_d - p\mathbf{I}]\cdot\mathbf{n} + \gamma(c)\kappa\mathbf{n} - \nabla_s\gamma(c)\Big\}\,\mathrm{d}A + \int_{\Gamma(t)}e''(c)\nabla_s c\cdot\mathbf{J}_c\,\mathrm{d}A\\ &+\int_{\Lambda}u_l\Big\{\gamma(c)\cos\theta_d + (\gamma_1-\gamma_2)\Big\}\,\mathrm{d}l,\end{aligned} \tag{27}$$

where u_l is the normal velocity of the contact line: $u_l = \mathbf{u}\cdot\mathbf{n}_l$, θ_d is the dynamic contact angle, and we have used the identity $\mathbf{u}\cdot\mathbf{n}_s = u_l\cos\theta_d$.

The above result reveals four different dissipation mechanisms for the free energy of the system: the rate of energy dissipation in the bulk of the fluids due to the viscous force (the first term), on the solid surface (the second term), on the fluid interface (the third and fourth terms), and at the moving contact line (the last term), respectively. The second law of thermodynamics asserts that $\mathrm{d}F/\mathrm{d}t \leq 0$. Here we make a stronger assumption, requiring each term in (27) be non-positive. This places

constraints on the constitutive relations for the slip velocity $\mathbf{u}_s$, the normal velocity of the contact line u_l, and the mass flux of the surfactant $\mathbf{J}_c$, as follows:

1. On the fluid interface $\Gamma(t)$, we assume no dissipation occurs except for that induced by $\mathbf{J}_c$. Thus we set the third term in (27) to zero and obtain the interface condition:

$$[\tau_d - p\mathbf{I}] \cdot \mathbf{n} = -\gamma(c)\kappa\mathbf{n} + \nabla_s\gamma(c), \tag{28}$$

   where the last term is known as the Marangoni force. This is a force balance equation as described by Edwards *et al.*[39] The rate of energy dissipation due to the motion of the surfactant is characterized by the fourth term in (27). This needs to be non-positive, which places a constraint on the mass flux $\mathbf{J}_c$:

$$e''(c)\nabla_s c \cdot \mathbf{J}_c \leqslant 0. \tag{29}$$

2. The form of the energy dissipation on the solid surface leads to the slip boundary condition for the fluid velocity:

$$\mathcal{P}(\tau_d \cdot \mathbf{n}_b) = \mathbf{f}_i(\mathbf{u}_s), \quad \text{on } \Gamma_i, \tag{30}$$

   where the map $\mathbf{f}_i : \mathbb{R}^2 \to \mathbb{R}^2$ satisfies

$$\mathbf{u} \cdot \mathbf{f}_i(\mathbf{u}) \leqslant 0, \qquad \forall\, \mathbf{u} \in \mathbb{R}^2. \tag{31}$$

3. The form of the energy dissipation at the contact line gives the condition for the dynamic contact angle θ_d:

$$\gamma(c)\cos\theta_d + (\gamma_1 - \gamma_2) = f_{CL}(u_l), \tag{32}$$

   where the function $f_{CL}(u)$ satisfies

$$u f_{CL}(u) \leqslant 0, \quad \forall\, u \in \mathbb{R}. \tag{33}$$

In summary, from the consideration of energy dissipations, we obtained the conditions (28), (30), and (32) on the fluid interface, on the solid surface, and at the moving contact line, respectively, with the constraints (29), (31), and (33) on the constitutive relations. With the dynamical equations (18) and [(21a) and (21b)], the no-flux boundary condition (19) for the surfactant, and the usual no-penetration condition (26), these form the continuum model for the dynamics of the system.

C. Linear constitutive relations, Langmuir equation of state, and the energy law

The continuum model derived in Sec. III B contains the constitutive relations for the friction forces $\mathbf{f}_i(\mathbf{u})$ and $f_{CL}(u)$, the energy density of the fluid interface $e(c)$, and the mass flux of the surfactant $\mathbf{J}_c$. These constitutive relations need to be calibrated from other means, e.g., by fitting experimental data or "first-principle" simulations such as molecular dynamics. Below we give simple examples for these functions which satisfy the constraints (29), (31), and (33).

When the slip velocity is not too large, it is expected that the linear response theory holds on the fluid-solid interface, thus we may approximate $\mathbf{f}_i$ and f_{CL} in (30) and (32) using linear functions,

$$\mathbf{f}_i(\mathbf{u}) = -\beta_i\mathbf{u}, \quad f_{CL}(u) = -\beta_{CL}u, \tag{34}$$

where β_i and β_{CL} are the friction coefficients on the fluid-solid interface and at the contact line, respectively. This leads to the boundary condition for the slip velocity,

$$\eta_i\partial_n\mathbf{u}_s = -\beta_i\mathbf{u}_s, \quad \text{on } \Gamma_i, \tag{35}$$

where ∂_n denotes the derivative in the outward normal direction to the wall, and the condition for the dynamic contact angle:

$$\gamma(c)\cos\theta_d + (\gamma_1 - \gamma_2) = -\beta_{CL}u_l. \tag{36}$$

Equation (35) is the Navier slip condition. Equation (36) provides a relation between the dynamic contact angle and the normal velocity of the contact line.

Turning to the surface tension of the fluid interface, the energy density $e(c)$ can be written as the sum of γ^0, the density of the free energy of a clean interface, and the contribution from the entropy of mixing due to the addition of the surfactant,

$$e(c) = \gamma^0 + RTc_\infty \left(\frac{c}{c_\infty} \ln \frac{c}{c_\infty} + \left(1 - \frac{c}{c_\infty}\right) \ln \left(1 - \frac{c}{c_\infty}\right) \right), \tag{37}$$

where R is the ideal gas constant, T is the temperature, and c_∞ is the surfactant concentration at maximum packing. Then using the definition of the surface tension, Eq. (9), we obtain

$$\gamma(c) = \gamma^0 + RTc_\infty \ln \left(1 - \frac{c}{c_\infty}\right). \tag{38}$$

This is the Langmuir equation of state for the surface tension, which has been widely used in the literature.[1–3]

It is easy to check that the second order derivative of the energy density (37) is positive for all $0 < c < c_\infty$:

$$e''(c) = \frac{RTc_\infty}{c(c_\infty - c)} > 0. \tag{39}$$

Then the conventional Fick's law for the mass flux $\mathbf{J}_c$, given by

$$\mathbf{J}_c = -D\nabla_s c, \tag{40}$$

is a particular form of the flux which satisfies the constraint (29). Here $D > 0$ is the diffusivity of the surfactant, which is assumed to be a constant in this work.

Using the interface condition (28), the constitutive relations (35) and (36) for the friction forces on the solid wall, (37) for the energy density of the interface, and (40) for the mass flux of the surfactant, the energy law (27) becomes

$$\begin{aligned} \frac{\mathrm{d}F}{\mathrm{d}t} = &- \sum_{i=1,2} \int_{\Omega_i} \eta_i \left|\nabla \mathbf{u}\right|^2 \mathrm{d}\mathbf{x} - \sum_{i=1,2} \int_{\Gamma_i} \beta_i \left|\mathbf{u}_s\right|^2 \mathrm{d}A - \int_\Lambda \beta_{CL} u_l^2 \,\mathrm{d}l \\ &- \int_{\Gamma(t)} De''(c) \left|\nabla_s c\right|^2 \,\mathrm{d}A. \end{aligned} \tag{41}$$

IV. NUMERICAL EXAMPLES

A. Dimensionless equations

In numerical simulations, it is more convenient to solve the equations in their dimensionless form. To make the variables dimensionless, we rescale the density ρ_i, the viscosity η_i, and the friction coefficient β_i using their values in fluid 2: ρ_2, η_2, and β_2, respectively. The friction coefficient at the contact line β_{CL} has the dimension of viscosity, thus we rescale it using η_2. The surface tensions are rescaled using γ^0, the surface tension of the clean interface. Other quantities are made dimensionless in the usual way. Specifically, we define

$$\hat{\rho}_i = \frac{\rho_i}{\rho_2},\ \hat{\eta}_i = \frac{\eta_i}{\eta_2},\ \hat{\beta}_i = \frac{\beta_i}{\beta_2},\ \hat{\beta}_{CL} = \frac{\beta_{CL}}{\eta_2},\ \hat{\gamma}_i = \frac{\gamma_i}{\gamma^0},\ \hat{\gamma} = \frac{\gamma}{\gamma^0},$$

$$\hat{\mathbf{x}} = \frac{\mathbf{x}}{L},\ \hat{t} = \frac{Ut}{L},\ \hat{\mathbf{u}} = \frac{\mathbf{u}}{U},\ \hat{p} = \frac{p}{\rho_2 U^2},\ \hat{\kappa} = L\kappa,$$

then the Navier-Stokes equations in the bulk Ω_i become (dropping hats)

$$\rho_i \left(\partial_t \mathbf{u} + (\mathbf{u}\cdot\nabla)\mathbf{u}\right) = -\nabla p + \frac{1}{Re}\nabla\cdot\tau_d, \tag{42a}$$

$$\nabla\cdot\mathbf{u} = 0, \tag{42b}$$

where $\tau_d = \eta_i\left(\nabla\mathbf{u} + (\nabla\mathbf{u})^\top\right)$. The interface condition becomes

$$We\left[\frac{1}{Re}\tau_d - p\mathbf{I}\right]\cdot\mathbf{n} = -\gamma(c)\kappa\mathbf{n} + \nabla_s\gamma(c) \tag{43}$$

on the fluid interface Γ. The slip boundary condition on Γ_i is

$$-\beta_i\mathbf{u}_s = \eta_i l_s \partial_n \mathbf{u}_s, \tag{44}$$

and the condition for the dynamic contact angle is

$$-\beta_{CL}u_l = \frac{1}{Ca}\big(\gamma(c)\cos\theta_d + (\gamma_1 - \gamma_2)\big). \tag{45}$$

In the above equations, we have used the linear constitutive relations given in Sec. III C. The Reynolds number Re, the Capillary number Ca, the Weber number We, and the slip length l_s are defined as follows:

$$Re = \frac{\rho_2 UL}{\eta_2},\ Ca = \frac{\eta_2 U}{\gamma^0},\ We = Re\cdot Ca,\ l_s = \frac{\eta_2}{\beta_2 L}.$$

For the surfactant equation, we rescale the concentration c using c_∞, the value at the maximum packing. Using the linear constitutive relation (40) for the mass flux, we obtain the convection-diffusion equation

$$\frac{\mathrm{D}c}{\mathrm{D}t} + (\nabla_s\cdot\mathbf{u})c = \frac{1}{Pe}\nabla_s^2 c, \tag{46}$$

with the boundary condition

$$\nabla_s c\cdot\mathbf{n}_s = 0. \tag{47}$$

In (46), Pe is the Péclet number

$$Pe = LU/D.$$

Finally, the dimensionless Langmuir equation of state is given by

$$\gamma(c) = 1 + k\ln(1-c), \tag{48}$$

where $k = RTc_\infty/\gamma^0$ is the surfactant elasticity. The fluid surface Γ evolves according to the velocity field $\mathbf{u}$:

$$\dot{\mathbf{x}} = \mathbf{u}(\mathbf{x}, t). \tag{49}$$

In terms of the dimensionless variables, the free energy (20) becomes

$$F = \sum_{i=1,2}\int_{\Omega_i}\frac{1}{2}\rho_i|\mathbf{u}|^2\,\mathrm{d}\mathbf{x} + \frac{1}{We}(\gamma_1-\gamma_2)|\Gamma_1| + \frac{1}{We}\int_{\Gamma(t)} e(c)\,\mathrm{d}A, \tag{50}$$

where we have rescaled the free energy using $\rho_2 U^2 L^3$. The energy law (27) in its dimensionless form reads

$$\frac{\mathrm{d}F}{\mathrm{d}t} = \dot{F}_b + \dot{F}_s + \dot{F}_l + \dot{F}_c, \tag{51}$$

where the four terms are the rate of energy dissipation in the bulk ($\dot{F}_b$), on the solid surface ($\dot{F}_s$), at the contact line ($\dot{F}_l$), and due to the diffusion of the surfactant ($\dot{F}_c$), respectively. With the linear constitutive relations, they are given by

$$\dot{F}_b = -\sum_{i=1,2}\frac{1}{Re}\int_{\Omega_i}\eta_i|\nabla\mathbf{u}|^2\,\mathrm{d}\mathbf{x}, \tag{52a}$$

$$\dot{F}_s = -\sum_{i=1,2} \frac{1}{Re \cdot l_s} \int_{\Gamma_i} \beta_i u_s^2 \, \mathrm{d}A, \tag{52b}$$

$$\dot{F}_l = -\frac{1}{Re} \int_{\Lambda} \beta_{CL} u_l^2 \, \mathrm{d}l, \tag{52c}$$

$$\dot{F}_c = -\frac{1}{We \cdot Pe} \int_{\Gamma(t)} e''(c) |\nabla_s c|^2 \, \mathrm{d}A, \tag{52d}$$

where in the last equation $e''(c) = k/c(1-c)$.

The above continuum model contains the following parameters: the ratios of the densities, the viscosities, the friction coefficients of the two fluids, the ratio of the friction coefficient at the contact line to the viscosity, the difference of the surface tensions $\gamma_1 - \gamma_2$, the Reynolds number, the Capillary number, the slip length, the Péclet number, and the surfactant elasticity in the Langmuir equation of state. In the following numerical examples, we consider two fluids of similar properties in the mesoscopic scale. Unless otherwise stated, the two fluids have equal density and equal viscosity, $Re = 10$, $Ca = 0.1$, $Pe = 10$, $l_s = 0.1$, and $k = 1$. For the dimensionless friction coefficients, we choose $\beta_1 = \beta_2 = \beta_{CL} = 1$. Other parameters are specified in the examples.

B. Numerical method

In the numerical examples presented below, we consider the relaxation dynamics of a two-dimensional droplet. We also assume the Reynolds number is small so we neglect the inertia term in the Navier-Stokes equations and solve the time-independent Stokes equation for the flow field.

The Stokes equation is solved using the finite element method with unstructured elements in the domains Ω_1 and Ω_2. An example of the triangulation is shown in Fig. 3. In this work, we use the standard P_2-P_1 element to solve the coupled saddle point problem for the Stokes equation. The fluid interface is represented by a number of markers. These markers are also the nodes of the triangular elements neighboring the interface. The convection-diffusion equation for the surfactant is solved using the finite element method, on the mesh formed by the markers on the interface.

The overall procedure of the numerical method is as follows. At each time step, the velocity field is first solved using the current distribution of the surfactant on the interface. Then the fluid interface, except the contact points which are moved according to the relation (45), are updated according to the velocity field. For a better representation of the interface, the markers are redistributed at each time step according to the equal-arclength parametrization so that they are evenly distributed on the interface. After the redistribution of the markers, the surfactant concentration on the new mesh is obtained from interpolation using the values on the old mesh. The surfactant concentration is finally updated by solving the diffusion equation on the new mesh.

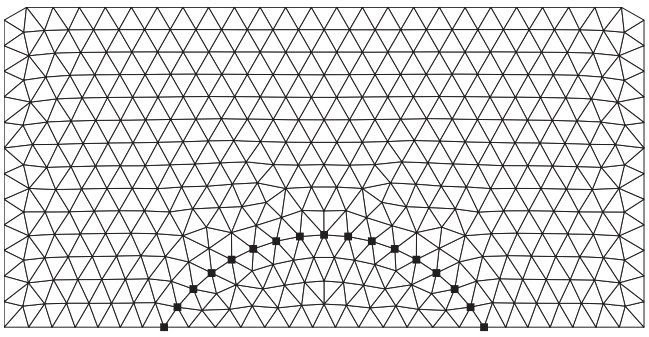

FIG. 3. Triangulation of the computational domain and the fluid interface. The interface is represented by markers indicated by the solid dots. The markers are also the nodes of the triangular mesh on the interface.

To assess the accuracy and convergence of the numerical method, we consider the dynamics of a droplet driven by the diffusion of surfactant and the Marangoni force. Initially, the droplet is in its static state with no surfactant on its interface. The interface is given by a spherical cap with the equilibrium contact angle $\theta_Y = 60^\circ$ and the radius 0.5. This is the static configuration, so without external force, the droplet will stay unchanged.

At $t = 0$, we add certain amount of surfactant to the interface. Specifically, the surfactant concentration is $c = 0.4$ on the left half of the interface, and $c = 0.2$ on the right half of the interface. Then the surfactant starts to diffuse from the left to the right, and the Marangoni force due to the uneven distribution of the surfactant generates a velocity field which drives the system to a new equilibrium state. A slip velocity is also generated at the contact points due to the change of the surface tension $\gamma(c)$.

The computational domain is $[-1, 1] \times [0, 1]$. The periodic boundary condition is used in the x direction. The velocity at the upper boundary is fixed at $\mathbf{u} = 0$. To test the convergence of the numerical method, we use different mesh sizes: $h = 0.08$, 0.04, 0.02, and 0.01, respectively. Correspondingly, we use $N_s = 17$, 31, 61, and 121 nodes on the interface. This makes the mesh size of the surface element also of the order $O(h)$. The trajectories of the two contact points are shown in Fig. 4. It is evident that the numerical results converge as we refine the mesh.

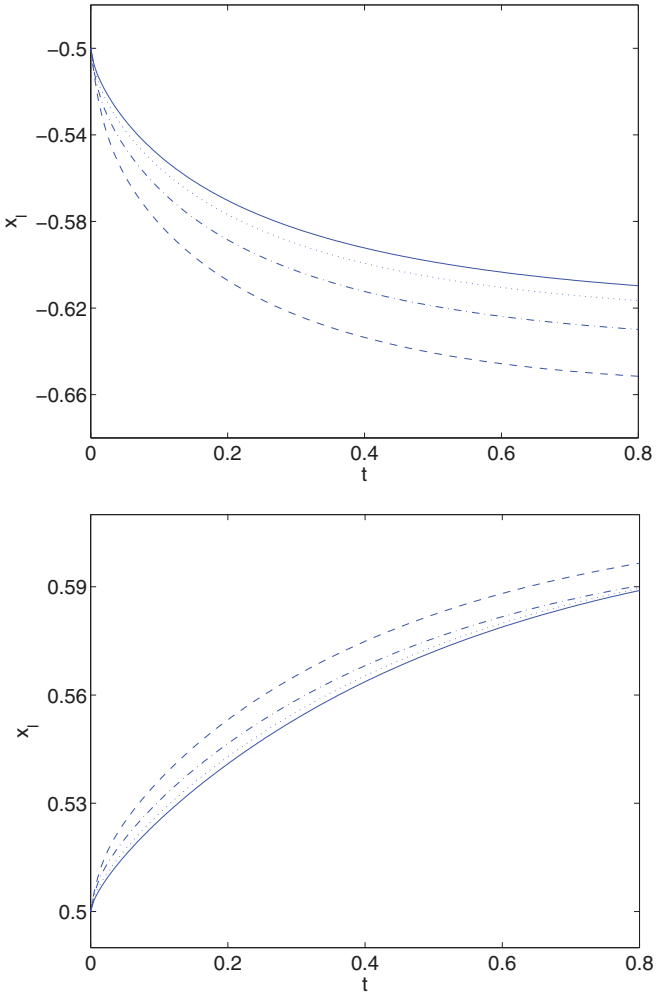

FIG. 4. Displacement of the left contact point (upper panel) and the right contact point (lower panel). The different curves are obtained using different mesh sizes: $h = 0.08$ (dashed curve), 0.04 (dashed-dotted curve), 0.02 (dotted curve), and 0.01 (solid curve).

Moreover, the numerical results show that the accuracy for the velocity filed and the surfactant concentration is about order 1.5. The discrepancy from the theoretical second-order accuracy of the P_2-P_1 element is possibly because of the linear-segment approximation of the interface and the curvature. Details on the dynamics of the droplet and the evolution of the surfactant are given in Sec. IV C.

C. Droplet dynamics driven by addition of surfactant

In this example, we consider the detailed dynamics of the system used in the convergence test. Recall that the droplet is in the static state with the contact angle $\theta_Y = 60^\circ$ initially. The surfactant concentration is suddenly increased from $c = 0$ to $c = 0.4$ and $c = 0.2$ on the left and right half

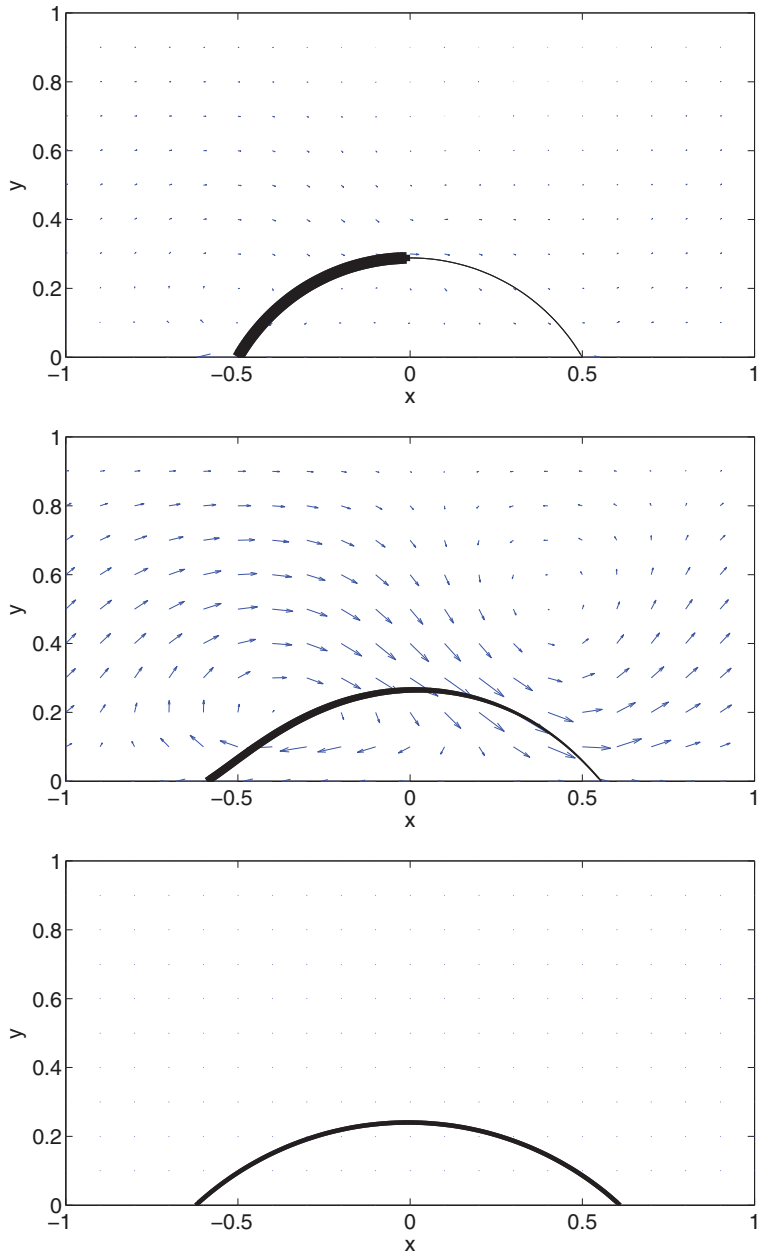

FIG. 5. The droplet profile and the velocity field at $t = 0$ (upper panel), 0.3 (middle panel), and 10 (lower panel) after adding the surfactant to the static droplet. The thickness of the interface indicates the concentration of the surfactant.

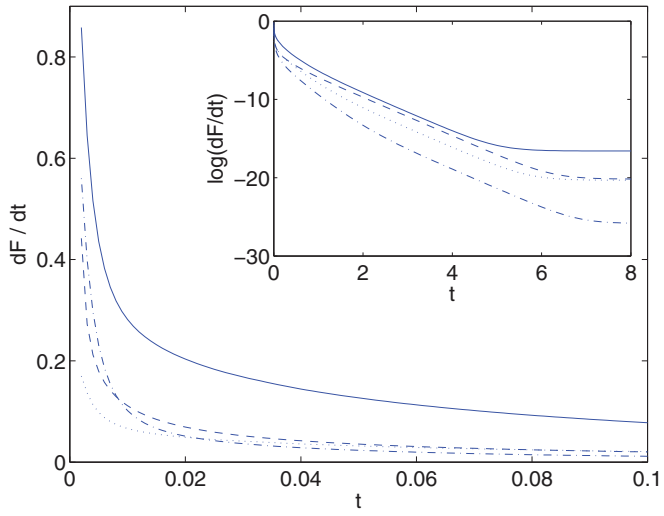

FIG. 6. Comparison of the different types of energy dissipations (in absolute values): Viscous dissipation (solid curve), dissipation on the solid wall (dotted curve), dissipation at the contact line (dashed-dotted curve), dissipation on the fluid interface (dashed curve). The inset shows that the dissipations decay exponentially.

of the interface, respectively. This changes the surface tension of the fluid interface, which drives the droplet to a new equilibrium. In the simulation, the size of the elements is $h = 0.02$. We use $N_s = 61$ nodes on the interface. The time step is $\Delta t = 0.001$.

As shown in Fig. 5 (upper panel), immediately after the addition of the surfactant, velocities are generated at the two contact points due to the change of the surface tension $\gamma(c)$. The droplet starts to spread. Moreover, due to the jump of the distribution of the surfactant in the middle of the interface, a Marangoni force is generated. This in turn generates a velocity field in the bulk of the fluids. The surfactant starts to diffuse along the interface, while the interface itself evolves according to the velocity field.

The configuration of the droplet and the velocity field at a later time ($t = 0.3$) is shown in the middle panel of Fig. 5. The interface has departed from its initial profile. It becomes asymmetric due to the diffusion of the surfactant from the left to the right. The left contact point moves further than the right one and the left contact angle undergoes a larger change. Due to the non-uniform distribution of the surfactant, the velocity field is relatively large near the middle of the interface. After reaching the new equilibrium, as shown in Fig. 5 (lower panel), the surfactant distribution becomes uniform with concentration $c = 0.265$. Because of the change of the local surface tension $\gamma(c)$, the equilibrium contact angle is lowered to 41.9°. Compared to the initial configuration, the center of the droplet moved to the left slightly.

The four types of energy dissipations are compared in Fig. 6. All dissipations are large at the very beginning. The viscous dissipation in the bulk dominates the others. The initial large dissipation at the contact line is an evidence that the dynamics is driven by the contact line motion at the beginning. At later times, the dissipation due to the diffusion of the surfactant becomes more important than the dissipation at the contact line. These dissipations decay exponentially as shown in Fig. 6 (inset).

D. Relaxation dynamics of a droplet

In this example, we consider the relaxation of a droplet to its equilibrium state. In particular, we compare the dynamics of a clean interface with the dynamics of an interface with surfactants.

Initially, the interface is given by a semi-circle of radius 0.5 and with the contact angle 90°. In the simulation, the mesh and the time step are the same as used in the previous example. First we consider a clean interface without surfactants. The equilibrium contact angle of the clean interface

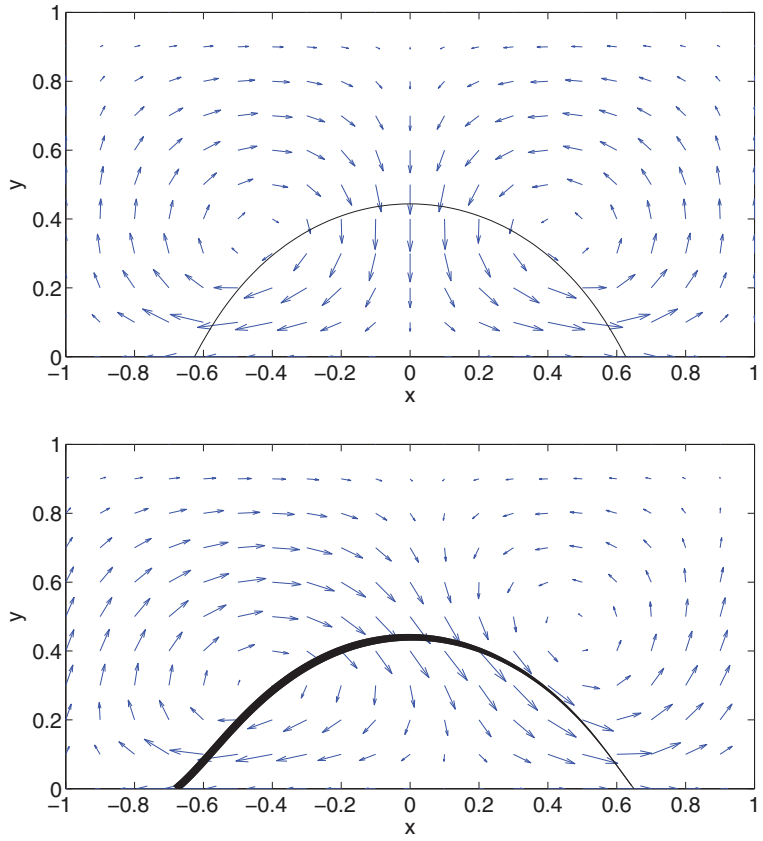

FIG. 7. Velocity field and the droplet profile of the clean interface (upper panel) and the interface with surfactant (lower panel) at $t = 0.3$ on a hydrophilic surface. The thickness of the curve indicates the surfactant concentration.

is $\theta_Y = 60^\circ$. A velocity field is generated at the contact lines because of the unbalanced Young stress (the right-hand side of (45)). The contact lines move outwards and the droplet begins to spread on the solid surface. The velocity field at time $t = 0.3$ is shown in Fig. 7 (upper panel). Two vortices are generated near the interface. The steady state of the interface is shown in Fig. 8 (solid curve). At the steady state, the interface takes the shape of a spherical cap and the contact angle reaches the equilibrium value 60°.

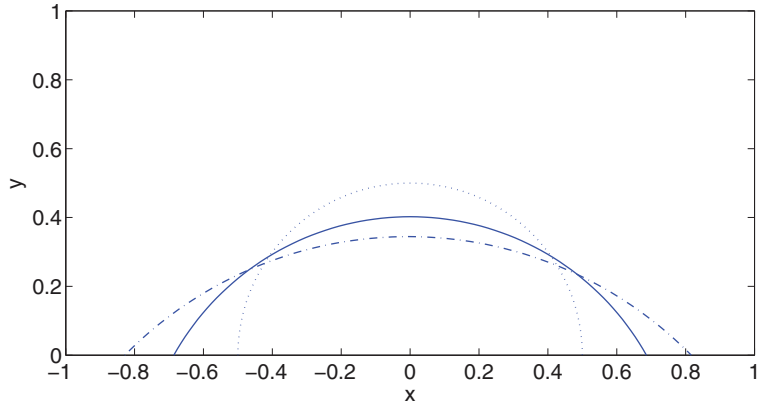

FIG. 8. Comparison of the profile of the clean interface (solid curve) and the interface with surfactant (dashed curve) at the steady state. The initial interface is given by the dotted curve. Due to the lowered surface tension by the addition of surfactant, the droplet spreads further compared to the clean interface.

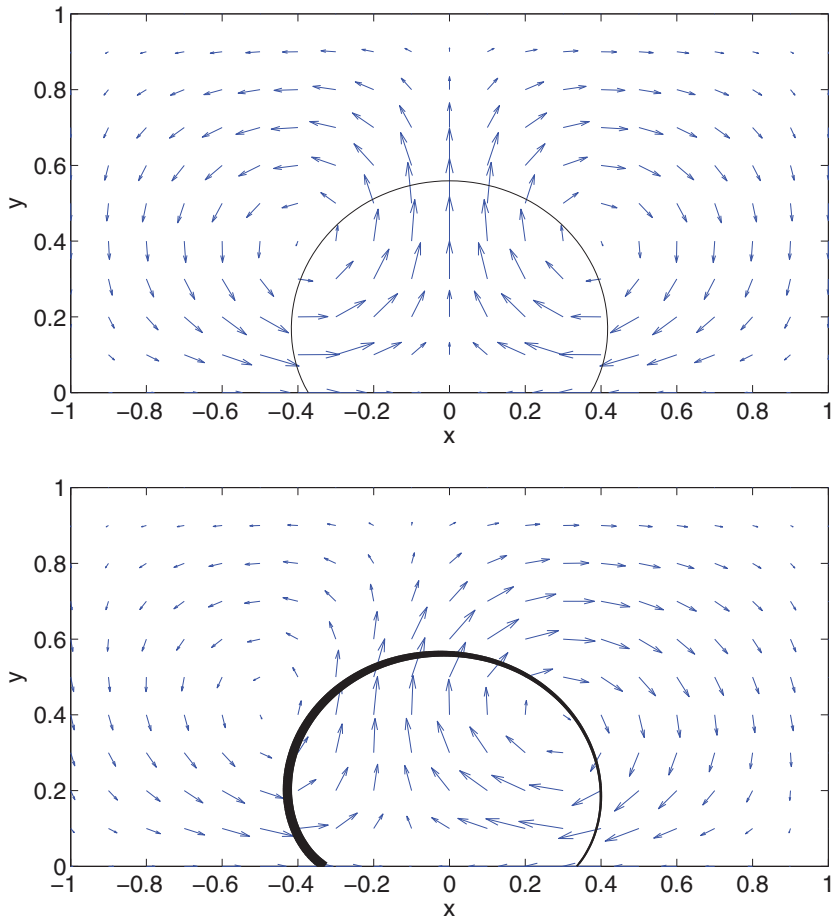

FIG. 9. Velocity field and the droplet profile of the clean interface (upper panel) and the interface with surfactant (lower panel) at $t = 0.3$ on a hydrophobic surface. The thickness of the curve indicates the surfactant concentration.

Next we consider the droplet dynamics in the presence of surfactant. Initially, the surfactant concentration is $c = 0.4$ on the left half of the interface and $c = 0.2$ on the right half of the interface. Then besides the velocities generated at the contact points by the unbalanced Young stress, a nonzero velocity field is also generated in the middle of the interface due to the uneven distribution of the surfactant and the resulting Marangoni force. This can be observed in Fig. 7 (lower panel). The velocity field becomes asymmetric and is tilted toward the right contact point, following the concentration gradient along the interface. The spreading of the droplet is accelerated by the addition of the surfactant. The droplet also spreads further due to the lowered surface tension. At the steady state, the surfactant becomes uniformly distributed with concentration $c = 0.255$, and the equilibrium contact angle becomes 44.9°. This is shown in Fig. 8 (dashed curve).

On the contrary, the droplet recoils on a hydrophobic surface. The instantaneous velocity field for the case of clean surface at $t = 0.3$ is shown in Fig. 9 (upper panel). The static contact angle in this case is $\theta_Y = 120°$. Two symmetric vortices are also generated near the surface and the contact lines recede. At the steady state, the droplet takes a circular shape and the contact angle reaches the static contact angle, as shown in Fig. 10 (solid curve). The addition of surfactant has a similar effect on the dynamics as in the hydrophilic case. It leads to the acceleration of the contact line dynamics. The asymmetry of the velocity field due to the uneven distribution of the surfactant is also observed as in Fig. 9 (lower panel). At the steady state, the surfactant becomes uniformly distributed with concentration $c = 0.264$, and the static contact angle is increased to 136°.

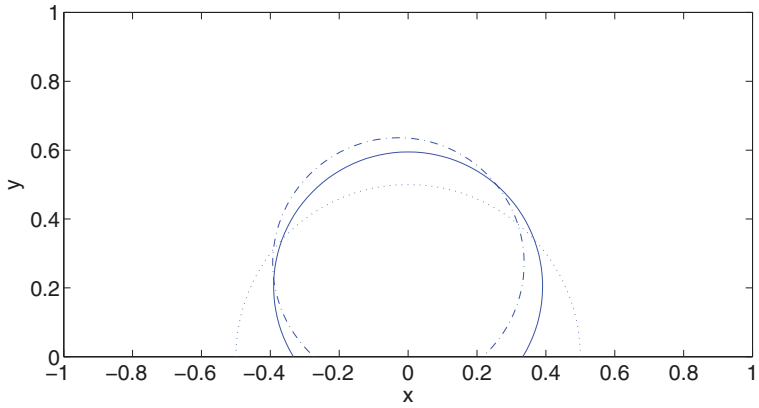

FIG. 10. Comparison of the profile of the clean interface (solid curve) and the interface with surfactant (dashed curve) at the steady state. The initial interface is given by the dotted curve. Due to the lowered surface tension by the addition of surfactant, the contact lines move further compared to the case of the clean interface.

V. CONCLUSION

In this work, we considered the dynamics of two immiscible fluids with insoluble surfactant, and derived continuum models for both the static case and the dynamical problem. In the static case, we derived the Young-Laplace equation for the fluid interface, the Young's relation for the contact line, and the equilibrium condition for the surfactant concentration by minimizing the free energy of the system. In the dynamic case, we obtained the continuum model, in particular, the interface condition, the boundary condition for the slip velocity, and the condition for the dynamic contact angle, from the consideration of thermodynamics. The dynamic model consists of the Navier-Stokes equations for the velocity field and a convection-diffusion equation for the surfactant. When the constitutive relations are linear, this model reduces to the one used in previous work.

We analyzed the energy law of the dynamical system and identified the different types of energy dissipations. The analysis shows that, in addition to the viscous dissipation in the bulk, the energy is also dissipated on the solid surface and at the moving contact line, as well as on the fluid interface due to the diffusion of surfactant.

We also developed a finite element method for the continuum model in 2d, and carried out numerical experiments to illustrate the influence of surfactant on the contact line dynamics. The numerical examples showed that the addition of surfactant accelerates the contact line dynamics, and changes the equilibrium configuration of the droplet due to the change of the surface tension. The four types of energy dissipations were compared numerically. In these examples, we only considered fluids of similar properties and slow dynamics. In applications to realistic systems, some of the parameters, such as the friction coefficients, need to be calibrated with experiments or more detailed microscopic (e.g., molecular dynamics) simulations.

The approach we used to derive the continuum model is rather general and should be useful for many other problems. In an ongoing work, we are studying the contact line dynamics with additives, e.g., polymers. This is inspired by experiments in which it was observed that the addition of even a small amount of soluble polymers can significantly alter the receding dynamics of the contact line. It is also important to develop numerical methods for the contact line model in 3d. We intend to pursue these issues in our future work.

ACKNOWLEDGMENTS

We are grateful to Chun Liu (Penn State) and Jie Liu (National University of Singapore) for helpful discussions. The work was supported in part by Singapore A*STAR SERC PSF grant Project No. 1321202071.

APPENDIX A: DERIVATION OF THE EQUILIBRIUM CONDITIONS

The equilibrium conditions (7a), (7b), and (8) are derived from the free energy (5) using the calculus of variations.[40,41] Let λ and μ be the Lagrange multipliers associated with the isoperimetric constraints (6a) and (6b), respectively. For isoperimetric problems, the Lagrange multipliers are constant. The Lagrangian can be written as

$$L = \int_{\Gamma_1} \mathcal{L}(z, z_x, z_y, c)\,\mathrm{d}x\mathrm{d}y, \tag{A1}$$

where

$$\mathcal{L} = (\gamma_1 - \gamma_2) + (e(c) - \mu c)J(z_x, z_y) + \lambda z. \tag{A2}$$

The Euler-Lagrange equations are given by

$$-\nabla \cdot \left(\frac{\partial \mathcal{L}}{\partial z_x}, \quad \frac{\partial \mathcal{L}}{\partial z_y}\right) + \frac{\partial \mathcal{L}}{\partial z} = 0, \tag{A3a}$$

$$\frac{\partial \mathcal{L}}{\partial c} = 0. \tag{A3b}$$

The minimization of (A1) is a variational problem with a moving boundary (the contact line Λ), thus variation with respect to the boundary must be taken into account. This leads to the boundary condition

$$\mathcal{L} - (\mathbf{n}_l \cdot \nabla z)\left(\mathbf{n}_l \cdot \left(\frac{\partial \mathcal{L}}{\partial z_x}, \quad \frac{\partial \mathcal{L}}{\partial z_y}\right)\right) = 0, \qquad \text{on } \Lambda. \tag{A4}$$

In the above equations, $\nabla = (\partial_x, \partial_y)$ is the two dimensional gradient operator.

Using the Lagrangian in (A2), equations in (A3) can be written as

$$\nabla \cdot \left(J(z_x, z_y)^{-1}(e(c) - \mu c)\left(z_x, z_y\right)\right) = \lambda, \tag{A5a}$$

$$e'(c) = \mu. \tag{A5b}$$

With the help of the second equation, the first equation can be simplified and gives (7a).

Similarly, the boundary condition (A4) can be written as

$$(\gamma_1 - \gamma_2) + (e(c) - e'(c)c)J(z_x, z_y)\left(1 - (\mathbf{n}_l \cdot \mathbf{n})^2\right) = 0, \tag{A6}$$

where the unit normal vectors $\mathbf{n}$ and $\mathbf{n}_l$ are defined in Fig. 2. Using the relations $\mathbf{n} \cdot \mathbf{n}_l = \sin\theta_Y$ and $J(z_x, z_y)^{-1} = \cos\theta_Y$ at the contact line, Eq. (A6) leads to the Young's equation (8).

APPENDIX B: SURFACE CALCULUS

Given a surface Γ with parametrization $\mathbf{x} = \mathbf{x}(s^1, s^2)$, the contravariant basis vectors $\{\mathbf{t}_1, \mathbf{t}_2\}$ for the tangent plane of the surface at any point are given by

$$\mathbf{t}_i = \frac{\partial \mathbf{x}}{\partial s^i}. \tag{B1}$$

The surface element is defined by

$$\mathrm{d}s^2 = h_{11}\mathrm{d}s^1\mathrm{d}s^1 + 2h_{12}\mathrm{d}s^1\mathrm{d}s^2 + h_{22}\mathrm{d}s^2\mathrm{d}s^2, \tag{B2}$$

where $h_{ij} = \mathbf{t}_i \cdot \mathbf{t}_j$ $(i, j = 1, 2)$ are the components of the surface metric tensor. The determinant of the tensor is $h = h_{11}h_{22} - h_{12}^2 = \|\mathbf{t}_1 \times \mathbf{t}_2\|^2$. The normal vector to the surface is then given by

$$\mathbf{n} = \frac{1}{\sqrt{h}}\mathbf{t}_1 \times \mathbf{t}_2. \tag{B3}$$

The surface gradient operator is defined by

$$\nabla_s = \mathbf{t}^1 \frac{\partial}{\partial s^1} + \mathbf{t}^2 \frac{\partial}{\partial s^2}, \tag{B4}$$

where the covariant basis vectors $\mathbf{t}^i$ $(i = 1, 2)$ form a reciprocal basis set with $\mathbf{t}^i \cdot \mathbf{t}_j = \delta_{ij}$, where δ_{ij} is the Kronecker delta function. A direct calculation gives the explicit form of $\mathbf{t}^i$:

$$\mathbf{t}^1 = \frac{1}{h}(h_{22}\mathbf{t}_1 - h_{12}\mathbf{t}_2), \quad \mathbf{t}^2 = \frac{1}{h}(h_{11}\mathbf{t}_2 - h_{12}\mathbf{t}_1). \tag{B5}$$

The surface divergence of the vector $\mathbf{F} = F^1\mathbf{t}_1 + F^2\mathbf{t}_2 + F^3\mathbf{n}$ can be expressed as

$$\nabla_s \cdot \mathbf{F} = \frac{1}{\sqrt{h}} \left\{ \frac{\partial(\sqrt{h}F^1)}{\partial s^1} + \frac{\partial(\sqrt{h}F^2)}{\partial s^2} \right\} + F^3\kappa, \tag{B6}$$

where $\kappa = \kappa_1 + \kappa_2$ is the mean curvature of the surface and κ_i $(i = 1, 2)$ are the two principal curvatures.

For a bounded surface Γ, we have surface divergence theorem analogous to the usual divergence theorem. Let $\mathbf{t}_s$ be the tangent vector to the boundary $\partial\Gamma$ in the anti-clockwise direction, and $\mathbf{n}_s = \mathbf{t}_s \times \mathbf{n}$ be the unit vector tangent to the surface Γ and normal to $\partial\Gamma$. By using the Stokes theorem, we obtain the surface divergence theorem for any vector $\mathbf{F}(s^1, s^2)$ defined on the surface:

$$\begin{aligned} \int_{\partial\Gamma} \mathbf{F} \cdot \mathbf{n}_s \mathrm{d}l &= \int_{\partial\Gamma} \mathbf{t}_s \cdot (\mathbf{n} \times \mathbf{F}) \mathrm{d}l = \int_{\Gamma} \mathbf{n} \cdot \nabla \times (\mathbf{n} \times \mathbf{F}) \mathrm{d}A \\ &= \int_{\Gamma} \mathbf{n} \cdot ((\nabla \cdot \mathbf{F})\mathbf{n} - (\nabla \cdot \mathbf{n})\mathbf{F} + (\mathbf{F} \cdot \nabla)\mathbf{n} - (\mathbf{n} \cdot \nabla)\mathbf{F}) \, \mathrm{d}A \\ &= \int_{\Gamma} (\nabla_s \cdot \mathbf{F} - 2\kappa \mathbf{F} \cdot \mathbf{n}) \mathrm{d}A, \end{aligned} \tag{B7}$$

where we have used $\nabla \cdot \mathbf{n} = \nabla_s \cdot \mathbf{n} = 2\kappa$, and the fact that $(\mathbf{F} \cdot \nabla)|\mathbf{n}|^2 = 0$ to eliminate $\mathbf{n} \cdot ((\mathbf{F} \cdot \nabla)\mathbf{n})$.

For the time derivative of the differential element, we have

$$\begin{aligned} \frac{\partial}{\partial t}\|\mathbf{t}_1 \times \mathbf{t}_2\| &= \frac{(\mathbf{t}_1 \times \mathbf{t}_2) \cdot (\frac{\partial \mathbf{t}_1}{\partial t} \times \mathbf{t}_2 + \mathbf{t}_1 \times \frac{\partial \mathbf{t}_2}{\partial t})}{\|\mathbf{t}_1 \times \mathbf{t}_2\|} \\ &= \frac{(\mathbf{t}_1 \times \mathbf{t}_2) \cdot (\frac{\partial \mathbf{u}}{\partial s^1} \times \mathbf{t}_2 + \mathbf{t}_1 \times \frac{\partial \mathbf{u}}{\partial s^2})}{\|\mathbf{t}_1 \times \mathbf{t}_2\|} \\ &= \frac{h_{22}\mathbf{t}_1 - h_{12}\mathbf{t}_2}{\sqrt{h}} \cdot \frac{\partial \mathbf{u}}{\partial s^1} + \frac{h_{11}\mathbf{t}_2 - h_{12}\mathbf{t}_1}{\sqrt{h}} \cdot \frac{\partial \mathbf{u}}{\partial s^2} \\ &= \sqrt{h}\left(\mathbf{t}^1 \cdot \frac{\partial \mathbf{u}}{\partial s^1} + \mathbf{t}^2 \cdot \frac{\partial \mathbf{u}}{\partial s^2}\right) = (\nabla_s \cdot \mathbf{u})\|\mathbf{t}_1 \times \mathbf{t}_2\|, \end{aligned} \tag{B8}$$

where $\mathbf{u}$ is the velocity, and we have used the Lagrange identity.

[1] J. Xu, Z. Li, J. Lowengrub, and H. Zhao, "A level-set method for interfacial flows with surfactant," J. Comput. Phys. **212**, 590–616 (2006).

[2] A. James and J. Lowengrub, "A surfactant-conserving volume-of-fluid method for interfacial flows with insoluble surfactant," J. Comput. Phys. **201**, 685–722 (2004).

[3] M. Lai, Y. Tseng, and H. Huang, "An immersed boundary method for interfacial flows with insoluble surfactant," J. Comput. Phys. **227**, 7279–7293 (2008).

[4] I. B. Bazhlekov, P. D. Anderson, and H. E. H. Meijer, "Numerical investigation of the effect of insoluble surfactants on drop deformation and breakup in simple shear flow," J. Colloid Interface Sci. **298**, 369–394 (2006).

[5] Y. Pawar and K. J. Stebe, "Marangoni effects on drop deformation in an extensional flow: The role of surfactant physical chemistry. I. Insoluble surfactants," Phys. Fluids **8**, 1738–1751 (1996).

[6] S. Khatri and A. K. Tornberg, "A numerical method for two phase flows with insoluble surfactants," Comput. Fluids **49**, 150–165 (2011).

[7] K. T. Teigen, P. Song, J. Lowengrub, and A. Voigt, "A diffuse-interface method for two-phase flows with soluble surfactants," J. Comput. Phys. **230**, 375–393 (2011).

[8] S. Yon and C. Pozrikidis, "Deformation of a liquid drop adhering to a plane wall: Significance of the drop viscosity and the effect of an insoluble surfactant," Phys. Fluids **11**, 1297–1308 (1999).
[9] R. Defay and I. Priogine, *Surface Tension and Adsorption* (Wiley, New York, 1966).
[10] D. I. Collias and R. K. Prudhomme, "Diagnostic techniques of mixing effectiveness: The effect of shear and elongation in drop production in mixing tanks," Chem. Eng. Sci. **47**, 1401–1410 (1992).
[11] H. P. Grace, "Dispersion phenomena in high viscosity immiscible fluid systems and application of static mixers as dispersion devices in such systems," Chem. Eng. Commun. **14**, 225–277 (1982).
[12] A. M. Schwartz, J. W. Perry, and J. Berch, *Surface Active Agents and Detergents* (Krieger, New York, 1977).
[13] P. Somasundaran and R. Ramachandran, "Surfactants in flotation," in *Surfactants in Chemical/Process Engineering*, edited by D. T. Wasan, M. E. Ginn, and D. O. Shah (Marcel Dekker, New York, 1988), Vol. 28, pp. 195–235.
[14] J. C. Baret, "Surfactants in droplet-based microfluidics," Lab Chip **12**, 422–433 (2012).
[15] A. Branger and D. Eckmann,"Accelerated arteriolar gas embolism reabsorption by an exogenous surfactant," Anesthesiology **96**, 971–979 (2002).
[16] D. M. Eckmann and V. N. Lomivorotov, "Microvascular gas embolization clearance following perfluorocarbon administration," J. Appl. Physiol. **94**, 860–868 (2003).
[17] T. Young, "An essay on the cohesion of fluids," Philos. Trans. R. Soc. London **95**, 65–87 (1805).
[18] C. Huh and L. E. Scriven, "Hydrodynamic model of steady movement of a solid/liquid/fluid contact line," J. Colloid Interface Sci. **35**, 85–101 (1971).
[19] E. B. Dussan V and S. H. Davis, "On the motion of a fluid-fluid interface along a solid surface," J. Fluid Mech. **65**, 71–95 (1974).
[20] E. B. Dussan V, "On the spreading of liquids on solid surfaces: Static and dynamic contact lines," Annu. Rev. Fluid Mech. **11**, 371–400 (1979).
[21] P. G. de Gennes, "Wetting: Statics and dynamics," Rev. Mod. Phys. **57**, 827–863 (1985).
[22] T. D. Blake, "The physics of moving wetting lines," J. Colloid Interface Sci. **299**, 1–13 (2006).
[23] D. Bonn, J. Eggers, J. Indekeu, J. Meunier, and E. Rolley, "Wetting and spreading," Rev. Mod. Phys. **81**, 739–805 (2009).
[24] P.-G. de Gennes, F. Brochard-Wyart, and D. Quéré, *Capillarity and Wetting Phenomena: Drops, Bubbles, Pearls, Waves* (Springer, New York, 2003).
[25] V. M. Starov, M. G. Velarde, and C. J. Radke, *Wetting and Spreading Dynamics* (CRC Press, Boca Raton, 2007).
[26] Y. D. Shikhmurzaev, *Capillary Flows with Forming Interfaces* (Chapman and Hall/CRC, Boca Raton, 2008).
[27] W. Ren, D. Hu, and W. E, "Continuum models for the contact line problem," Phys. Fluids **22**, 102103 (2010).
[28] W. Ren and W. E, "Derivation of continuum models for the moving contact line problem based on thermodynamic principles," Commun. Math. Sci. **9**, 597–606 (2011).
[29] H. Liu and Y. Zhang, "Phase-field modeling droplet dynamics with soluble surfactants," J. Comput. Phys. **229**, 9166–9187 (2010).
[30] J. Zhang, D. Eckmann, and P. Ayyaswamy, "A front tracking method for a deformable intravascular bubble in a tube with soluble surfactant transport," J. Comput. Phys. **214**, 366–396 (2006).
[31] M.-C. Lai, Y.-H. Tseng, and H. Huang, "Numerical simulation of moving contact lines with surfactant by immersed boundary method," Commun. Comput. Phys. **8**, 735–757 (2010).
[32] H. Stone, "A simple derivation of the time-dependent convective-diffusion equation for surfactant transport along a deforming interface," Phys. Fluids. A **2**, 111–112 (1990).
[33] H. Wong, D. Rumschitzki, and C. Maldarelli, "On the surfactant mass balance at a deforming fluid interface," Phys. Fluids **8**, 3203–3204 (1996).
[34] M. Muradoglu and G. Tryggvason, "A front-tracking method for computation of interfacial flows with soluble surfactants," J. Comput. Phys. **227**, 2238–2262 (2008).
[35] M. R. Booty and M. Siegel, "A hybrid numerical method for interfacial fluid flow with soluble surfactant," J. Comput. Phys. **229**, 3864–3883 (2010).
[36] K. Chen and M. Lai, "A conservative scheme for solving coupled surface-bulk convection-diffusion equations with an application to interfacial flows with soluble surfactant," J. Comput. Phys. **257**, 1–18 (2014).
[37] J. Xu and W. Ren, "A level-set method for two-phase flows with moving contact line and insoluble surfactant," J. Comput. Phys. **263**, 71–90 (2014).
[38] P. Cermelli, E. Fried, and M. Gurtin, "Transport relations for surface integrals arising in the formulation of balance laws for evolving fluid interfaces," J. Fluid Mech. **544**, 339–351 (2005).
[39] D. A. Edwards, H. Brenner, and D. T. Wasan, *Interfacial Transport Processes and Rheology* (Butterworth-Heinemann, 1991).
[40] B. von Brunt, *The Calculus of Variations* (Springer-Verlag, 2004).
[41] M. Giaquinta and S. Hildebrandt, *Calculus of Variations* (Springer, 1996), Vol. I and II.